Geochemical Perspectives Letters

Quantifying seawater exchange rates in the Eocene Arctic Basin using osmium isotopes

A.J. Dickson[1*], M. Davies[2,3], M.-L. Bagard[2,4], A.S. Cohen[2]

OPEN ACCESS

https://doi.org/10.7185/geochemlet.2239

Abstract

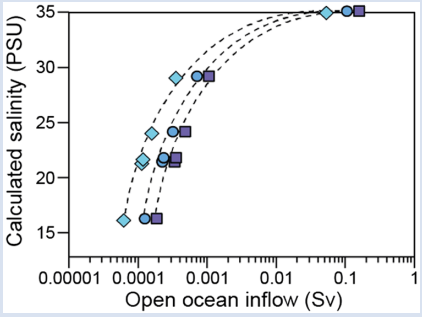

The closure of seaways that connected the Arctic Ocean to the global ocean during the early Paleogene led to severe hydrographic restriction. We present new osmium isotope data from organic-rich sediments deposited in the central Arctic Ocean during the Early–Middle Eocene. The new data show that the long term isotopic composition of osmium in Arctic seawater began to diverge from that of the global ocean at ~54 Ma, after the Eocene Thermal Maximum 2 hyperthermal event. This divergence was probably caused by the gradual closure of seaways connecting the Arctic Ocean to the global ocean. The Os data are used to calculate water exchange rates between the Arctic and surrounding oceans and to calculate Arctic Ocean salinity during the Early Eocene. The results show that the development of severe, long term Arctic Basin restriction after ~54 Ma occurred as open ocean seawater input decreased below ~0.01 Sv, resulting in a mean basin salinity between 8–16 PSU, depending on model assumptions.

Received 15 June 2022 | Accepted 28 September 2022 | Published 26 October 2022

Introduction

The Paleogene Arctic Ocean became hydrographically restricted in the Early to Middle Eocene due to both the closure of the Turgay Strait in northern Eurasia, and the progressive shoaling of the North Atlantic ridge, which probably acted as a valve for water exchange with the northern polar latitudes (Moran *et al.*, 2006; Stärz *et al.*, 2017; Fig. 1). By reducing the exchange of high salinity water, these tectonically driven events triggered a change to brackish/freshwater conditions in the basin during the late Early Eocene, as recorded by the well documented presence of the freshwater fern *Azolla* during the period ~49–48 Ma (Brinkhuis *et al.*, 2006). Oxygen, neodymium, and strontium isotope data indicate low salinity conditions (Waddell and Moore, 2008; Gleason *et al.*, 2009), which may have facilitated sea ice growth and an enhanced polar albedo effect in the middle Eocene (Stickley *et al.*, 2009). Reduced inflow of open ocean waters also caused the Arctic Ocean to evolve to anoxic-sulfidic depositional conditions, both over the long term duration of the Early–Middle Eocene (März *et al.*, 2010) and over shorter hyperthermal events such as the Paleocene–Eocene Thermal Maximum (Dickson *et al.*, 2012).

Despite being well characterised, the timing of hydrographic restriction in the Arctic Basin is uncertain (Moran *et al.*, 2006) and the water mass exchange rates that contributed to restricted conditions are not well quantified by hydrographic models (*e.g.*, Stärz *et al.*, 2017; Hutchinson *et al.*, 2019). Exchanges of heat and salt between the Arctic, Pacific, Atlantic and Tethys oceans would have been important factors controlling Eocene ocean circulation patterns and meridional heat transport, but model simulations disagree on the magnitude of circulation changes that may have been caused by progressive restriction (Roberts *et al.*, 2009; Cope and Winguth, 2011). In this contribution we present new osmium isotope measurements from IODP Site M0004A (Leg 302, 'ACEX' core). These measurements span the period 55.1–44.7 Ma and link the data published by Dickson *et al.* (2015, 2021) for the PETM and Eocene Thermal Maximum 2 (ETM-2) to the Middle Eocene (and younger) Os data published by Poirier and Hillaire-Marcel (2009, 2011). The new data are used as boundary conditions for a mass balance model that we use to quantify the flux of open ocean seawater into the Arctic Basin, and to quantify the mean Arctic Ocean salinities associated with these exchange rates.

Material and Methods

Sub-samples from Site M0004A between 205.43–345.48 mcd were oven dried and powdered. 1 g samples were digested at 180 °C for 5 days in 12 ml of inverse aqua regia in flame sealed Carius tubes following addition of a mixed ^{190}Os and ^{185}Re spike solution. Os was extracted from the chilled digest with CCl_4, then back extracted into HBr and micro-distilled using $Cr_{(VI)}$-H_2SO_4 (Cohen and Waters, 1996; Birck *et al.*, 1997). Solutions were loaded onto Pt filaments and analysed by negative thermal ionisation mass spectrometry. Os blanks were <1 pg (<1 % blank contribution) with an average $^{187}Os/^{188}Os$ ratio of 0.37. Precision of $^{187}Os/^{188}Os$ analyses was <0.2 % (2 s.d.), determined from a DTM Os standard

1. Centre of Climate Ocean and Atmosphere, Department of Earth Sciences, Royal Holloway University of London, Egham, Surrey, TW20 0EX, UK
2. Department of Environment, Earth and Ecosystems, The Open University, Milton Keynes, MK7 6AA, UK
3. School of Geography, Earth and Environmental Sciences, University of Plymouth, Plymouth, Devon, PL4 8AA, UK
4. Department of Earth Sciences, University of Cambridge, Downing Street, Cambridge, CB2 3EQ, UK
* Corresponding author (email: alex.dickson@rhul.ac.uk)

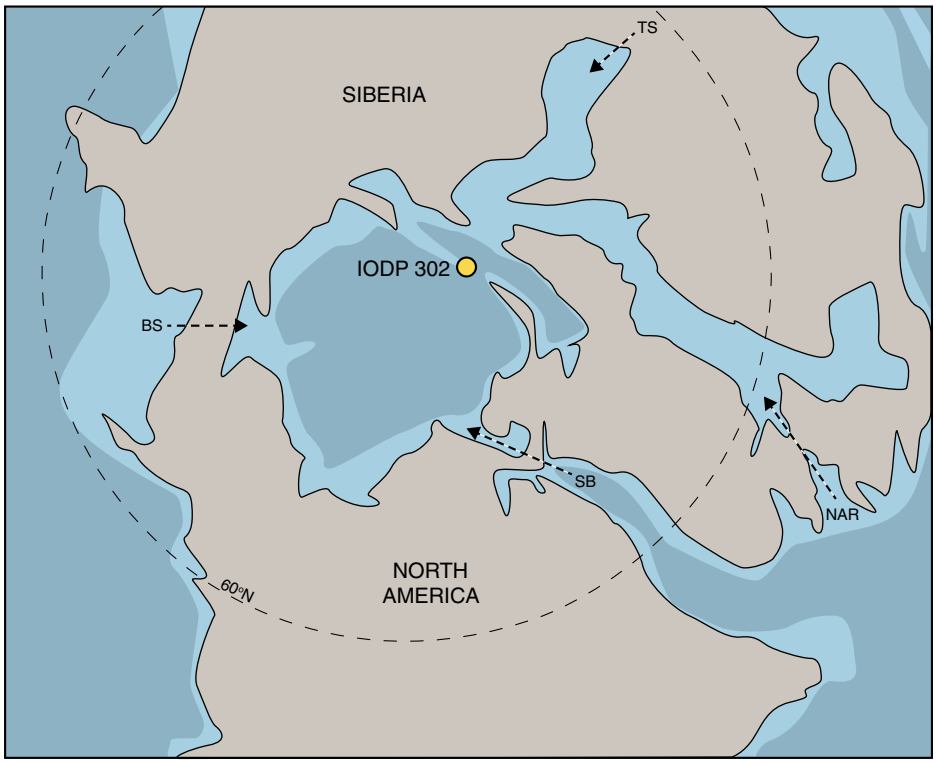

Figure 1 Palaeogeography of the Arctic region at *ca.* 50 Ma. Simplified map adapted from Blakey (2020). Oceanic straits allowing periodic exchanges of water into the Arctic are marked with arrows. TS: Turgay Strait. NAR: North Atlantic Ridge. BS: Bering Strait. SB: Sverdrup basin.

solution ($^{187}Os/^{188}Os = 0.17381 \pm 0.00104$, n = 14) and USGS SDO-1 ($^{187}Os/^{188}Os = 7.99404 \pm 0.00444$, n = 4). Re was partitioned from the acid digests into iso-amylol, back extracted into H_2O and analysed by MC-ICP-MS. Instrumental mass fractionation was corrected by the addition of 40 ppb Ir and normalising to a $^{193}Ir/^{191}Ir$ ratio of 1.68299. Re procedural blanks were <10 pg (blank contributions <0.02 %). Repeat digests of USGS SDO-1 gave an average Re concentration of 77.44 ± 1.83 ng/g (2 s.d., n = 6). Initial $^{187}Os/^{188}Os$ ratios ($^{187}Os/^{188}Os_i$) were calculated with a Re decay constant of 1.666 x 10^{-11} and a depositional age interpolated from the age model of Backman *et al.* (2008). The part of the ACEX core below ~300 mcd is not affected by the alternative age model of Poirier and Hillaire-Marcel (2009) but core levels above ~300 mcd would be progressively shifted to younger ages by up to 7 Myr. The choice of age model therefore has a small effect on the calculation of $^{187}Os/^{188}Os_i$ (Fig. S-1).

Results

$^{187}Os/^{188}Os_i$ range from 0.30–1.19 and become generally higher between ~55–45 Ma (Fig. 2, Table S-1). $^{187}Os/^{188}Os_i$ ratios overlap the values previously published by Poirer and Hillaire-Marcel (2011) for the upper part of the studied section. $^{187}Os/^{188}Os_i$ ratios in the lower part of the section are similar to those published for Eocene Thermal Maximum 2 (ETM-2) by Dickson *et al.* (2021). ^{192}Os concentrations reported here range from 28–86 pg/g and are notably lower than concentrations in older and younger Eocene sediments in the ACEX core (Fig. 2).

Arctic Ocean Restriction Identified using Os Isotope Data

Changes in the $^{187}Os/^{188}Os$ ratio of seawater are caused by the fractional mixing of continental-derived radiogenic and mantle-derived unradiogenic end members. Mixing ratios can be controlled in principle by increases or decreases in the flux of either end member, by processes typically linked to continental weathering and/or changing rates of submarine volcanic activity (Peucker-Ehrenbrink and Ravizza, 2000). In marginal marine basins, mixing ratios may also be controlled by the degree of water mass restriction, due to the variable input of open ocean seawater imprinted with unradiogenic Os from seafloor hydrothermal systems and basalt weathering (Dickson *et al.*, 2015). Such basins may become sensitised to local radiogenic Os fluxes. The behaviour of Os isotopes in marginal marine basins can therefore be used to quantify water mass mixing rates, where an Os isotope record from within a restricted basin can be robustly correlated to a time-equivalent open ocean Os isotope signature.

The Eocene Arctic Ocean satisfies these requirements because the near-continuous $^{187}Os/^{188}Os_i$ record reported in this study can be compared directly with open ocean Os isotope records obtained from ferromanganese crusts and metalliferous sediments (Peucker-Ehrenbrink *et al.*, 1995; Pegram and Turekian, 1999). This comparison, in Figure 2, shows that although there were transient episodes of divergence between the Arctic and global Os records in the early Eocene, such as during the PETM (Dickson *et al.*, 2015), the long term divergence in the records became pronounced after Eocene Thermal Maximum 2 (ETM2), at ~54 Ma. This divergence reached a maximum ~49–44 Ma, a period of time that brackets the *Azolla* interval and the occurrence of seasonal sea ice, both linked to fresher surface water conditions (Brinkhuis *et al.*, 2006; Stickley *et al.*, 2009). The Poirier and Hillaire-Marcel (2009) age model shifts the timing of maximum divergence ~2 Myr younger. The unique comparison of the Arctic record to records from open ocean ferromanganese crusts allows us to link this long term divergence in Os isotopes to the partial closure of circum-Arctic seaways, rather than to any large scale change in continental

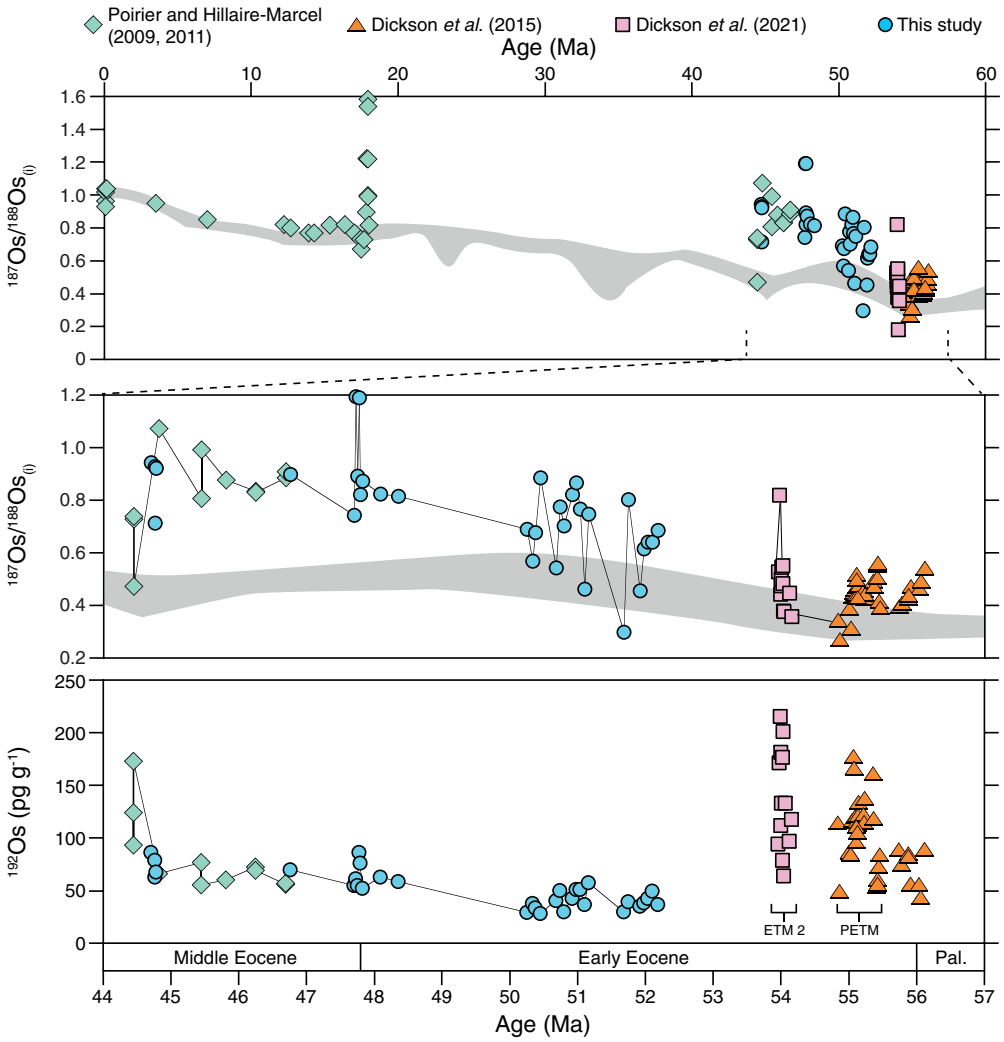

Figure 2 Initial osmium isotope ($^{187}Os/^{188}Os_i$) ratios and unradiogenic concentrations (^{192}Os, pg g^{-1}) of sediments deposited at IODP Site M0004A. The open ocean $^{187}Os/^{188}Os$ trend, taken from the ferromanganese crust data of Peucker-Ehrenbrink *et al.* (1995) and Pegram and Turkian (1999) is shown with grey shading. Published Os datasets are from Poirier and Hillaire-Marcel (2009, 2011) and Dickson *et al.* (2015, 2021). ETM 2: Eocene Thermal Maximum 2. PETM: Paleocene–Eocene Thermal Maximum. Pal: Paleocene.

weathering. The divergent Os isotope trends after 54 Ma are accompanied by relatively low Os concentrations (Fig. 2), which, given the associated transition to euxinic depositional conditions (März *et al.*, 2010), are likely related to basin scale trace metal depletion. The data contain deviations in $^{187}Os/^{188}Os_i$ that overlap with the open ocean trend (Fig. 2) which probably record ventilation events that punctuated the longer term transition to hydrographic restriction.

Quantifying Seawater Exchanges into the Arctic Basin

We have used the divergence of the Arctic Ocean and global Os isotope records (Fig. 2) to quantify the exchange rate of open ocean seawater into the Arctic Basin. In this approach, the mass accumulation rate of Os buried in the Arctic Basin is first estimated from typical early Eocene concentrations in Site M0004A of ~250 pg g^{-1} (this study and Poirier and Hillaire-Marcel, 2011), a dry bulk density of 1.4 g cm^{-3} (O'Regan, 2008) and an Eocene sediment accumulation rate of 0.002 cm yr^{-1} (Backman *et al.*, 2008). The mass accumulation rates of Os are scaled to an Eocene Arctic ocean area of 1.05×10^{17} cm^2 in order to calculate a total removal flux in pg yr^{-1}. This removal flux anchors subsequent quantification of the input fluxes to the Arctic Basin, by assuming mass balance.

The inputs of Os to the Arctic Basin come from two major sources: riverine discharge from pan-Arctic river systems and open ocean exchange through shallow seaways (North Atlantic/Fram Strait, Bering Strait, Turgay Strait). Riverine input fluxes are assigned a fixed $^{187}Os/^{188}Os$ of 1.4 (Peucker-Ehrenbrink and Jahn, 2001) and open ocean seawater $^{187}Os/^{188}Os$ is calculated as 2 million year averages of Fe/Mn-crust and metalliferous sediment data between 56–44 Ma (Table S-2). The magnitudes of each flux (f_{riv}, f_{sw}) are iteratively adjusted to obtain a match with the observed ACEX $^{187}Os/^{188}Os_i$, which is assumed to record Arctic seawater:

$$^{187}Os/^{188}Os_i = (f_{riv} * ^{187}Os/^{188}Os_{riv}) + (f_{sw} * ^{187}Os/^{188}O_{sw}) \quad \text{Eq.1}$$

These fractions (f_{riv}, f_{sw}) are scaled to the total Os removal mass for each 2 million year interval to obtain the mass of Os inputs (Os_{riv}, Os_{sw}), assuming approximate basin scale mass balance over the 2 million year calculation intervals. A key requirement is to simulate declining Arctic Ocean seawater concentrations with increasing basin restriction. Os_{riv} is thus held constant from the 56–54 Ma (most 'open') calculation, allowing declining values of Os_{sw} to cause a decline in Arctic seawater Os

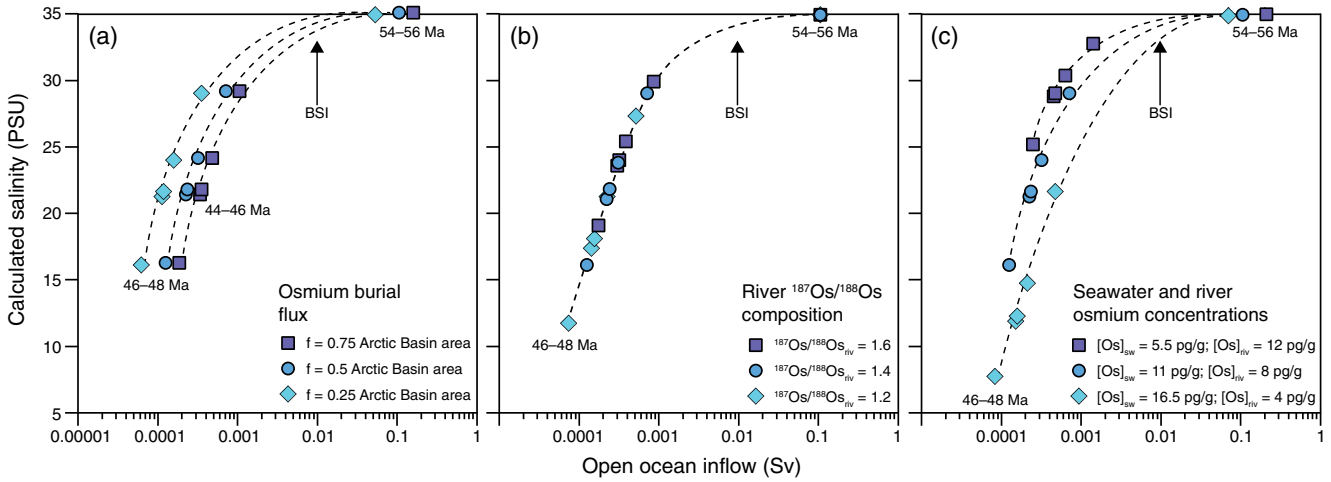

Figure 3 Calculated rates of open ocean seawater inflow to the Arctic Ocean, and Arctic Basin salinities. **(a)** Sensitivity tests of varying Os burial fluxes. **(b)** Sensitivity tests of varying pan-Arctic river compositions. **(c)** Sensitivity tests of varying the Os concentration in open ocean seawater and Arctic Rivers. BSI: modern Black Sea inflow of ~0.0097 Sv from Özsoy and Ünlüata (1997).

concentrations. A final step is to convert Os_{riv} and Os_{sw} to seawater volumes using ocean and river concentrations, initially assumed to be comparable to modern values of ~11 pg l^{-1} (Levasseur *et al.*, 1998) and ~8 pg l^{-1} (Levasseur *et al.*, 1999), respectively. f_{riv} *and* f_{sw} are used to calculate Arctic salinity by assigning end member values of ~0 PSU and ~35 PSU.

The effect of basin scale redox conditions on Os burial, basin size, sediment accumulation rates and sedimentary Os concentrations on the model are tested by varying Os burial rates. Other sensitivity tests include varying Arctic river $^{187}Os/^{188}Os$ ratios, a change that would affect f_{riv} and f_{sw}; and varying the concentrations of Os in open ocean seawater and Arctic river waters, parameters that affect the volumes of water (and hence seawater exchange rates) calculated from Os_{riv} and Os_{sw}. The calculations are illustrated in Figure 3 and documented in Tables S-3 to S-5.

Oceanic exchange rates are ~0.2 Sv for the Early Eocene (~56 Ma) and decline to a minimum of ~0.0001–0.0002 Sv by 48–46 Ma before increasing slightly by 46–44 Ma. The multi-million year divergent trend in $^{187}Os/^{188}Os$, which starts after ~54 Ma and parallels a switch to a persistently euxinic, silled Arctic Basin (März *et al.*, 2010), is accompanied by a decline in seawater exchange in all sensitivity tests to below ~0.01 Sv. This value is close to the modern exchange rate of Mediterranean seawater through the Bosphorus into the Black Sea (~0.0097 Sv; Özsoy and Ünlüata, 1997), where modern sediment $^{187}Os/^{188}Os$ ratios have also been characterised by mixing between seawater and local detrital end members (Ravizza *et al.*, 1991), and is ~1000 times lower than modern exchanges across the Fram Strait (Jakobsson *et al.*, 2007). Calculated Arctic salinities decrease to 7–25 PSU by 46–48 Ma, depending on the model conditions. This range is consistent with oxygen and strontium isotope salinity reconstructions of ~2–24 PSU for the same time interval (Waddell and Moore, 2008; Gleason *et al.*, 2009), but is higher than the ~1–6 PSU salinities required for the proliferation of *Azolla* ferns (Brinkhuis *et al.*, 2006). The discrepancy with the latter study is probably because the Os based estimates here are basin scale averages, whereas *Azolla* would typically colonise the upper, salinity stratified part of the water column. We note that the open ocean salinity end member used in the calculations is higher than modelled North Atlantic salinities under conditions of limited Arctic exchange (Roberts *et al.*, 2009; Stärz *et al.*, 2017). Lowering the marine end member to ~20 PSU further reduces the minimum Arctic Basin salinity during the period of maximum restriction (48–46 Ma) by 7–9 PSU across the various sensitivity tests. Use of the Poirier and Hillaire-Marcel (2009) ACEX age model does not significantly affect the magnitude of the hydrographic calculations, but shifts the timing of minimum salinity to younger ages by ~2 Myr.

Closure of the Arctic Ocean has been suggested as a cause of transient and/or persistent deep water overturning in the North Atlantic and North Pacific Oceans, due to a reduction in freshwater export to regions of overturning (Roberts *et al.*, 2009; Cope and Winguth, 2011; Hutchinson *et al.*, 2019). Our Os-based reconstruction of Arctic exchanges supports these ideas and provides quantitative constraints on water exchange rates. The use of Os isotope data to quantify hydrographic parameters can complement existing approaches to inferring basin hydrography using elemental proxies (Algeo and Lyons, 2006; Sweere *et al.*, 2016) but requires overcoming the hurdle of obtaining an open ocean Os isotope record that is time equivalent to one produced from a marginal basin. This goal may be difficult for some ancient time intervals for which deep ocean sedimentary deposits are not accessible. If the Eocene Arctic Ocean Os record were transposed, for example, into some distant part of Earth's history where an open ocean counterpart was lacking, the data might be incorrectly interpreted to represent a period of exaggerated continental weathering.

Acknowledgements

This study was funded by the Natural Environmental Research Council (NE/K006223/1).

Editor: Gavin Foster

Additional Information

Supplementary Information accompanies this letter at https://www.geochemicalperspectivesletters.org/article2239.

Cite this letter as: Dickson, A.J., Davies, M., Bagard, M.-L., Cohen, A.S. (2022) Quantifying seawater exchange rates in the Eocene Arctic Basin using osmium isotopes. *Geochem. Persp. Let.* 24, 7–11. https://doi.org/10.7185/geochemlet.2239

References

Algeo, T.J., Lyons, T.W. (2006) Mo-total organic carbon covariation in modern anoxic marine environments: implications for the analysis of colorredox and paleohydrologic conditions. *Paleoceanography and Paleoclimatology* 21, https://doi.org/10.1029/2004PA001112

Backman, J., Jakobsson, M., Frank, M., Sangiorgi, F., Brinkhuis, H., Stickley, C., O'Regan, M., Lvlie, R., Pälike, H., Spofforth, D., Gattacecca, J., Moran, K, King, J., Heil, C. (2008) Age model and core-seismic integration for the Cenozoic Arctic core expedition sediments from the Lomonosov Ridge. *Paleoceanography and Paleoclimatology* 23, PA1S03, http://doi.org/10.1029/2007PA001476

Birck, J-L., Roy Barman, M., Capmas, F. (1997) Re-Os measurements at the femtomole level in natural samples. *Geostandards Newsletter* 21, 19–27. http://doi.org/10.1111/j.1751-908X.1997.tb00528.x

Blakey, R. (2020) Paleotectonic and paleogeographic history of the Arctic region. *Atlantic Geology* 57, 7–39, http://doi.org/10.4138/atlgeol.2021.002

Brinkhuis, H., Schouten, S., Collinson, M.E., Sluijs, A., Sinninghe Damsté, J.S., Dickens, G.R., Huber, M., Cronin, T.M., Onodera, J., Takahashi, K., Bujak, J.P., Stein, R., van der Burgh, J., Eldrett, J.S., Harding, I.C., Lotter, A.F., Sangiorgi, F., van Konijnenburg-van Cittert, H., de Leeuw, J.W., Matthiessen, J., Backman, J., Moran, K., Expedition 302 Scientists (2006) Episodic fresh surface waters in the Eocene Arctic Ocean. *Nature* 441, 606–609. https://doi.org/10.1038/nature04692

Cohen, A.S., Waters, F.G. (1996) Separation of osmium from geological materials by solvent extraction for analysis by thermal ionisation mass spectrometry. *Analytica Chimica Acta* 332, 269–275. https://doi.org/10.1016/0003-2670(96)00226-7

Cope, J.T., Winguth, A. (2011) On the sensitivity of ocean circulation to arctic freshwater input during the Paleocene/Eocene Thermal Maximum. *Palaeogeography, Palaeoclimatology, Palaeoecology* 306, 82–94. https://doi.org/10.1016/j.palaeo.2011.03.032

Dickson, A.J., Cohen, A.S., Coe, A.L. (2012) Seawater oxygenation during the Paleocene-Eocene Thermal Maximum. *Geology* 40, 637–642, https://doi.org/10.1130/G32977.1

Dickson, A.J., Cohen, A.S., Coe, A.L., Davies, M., Shcherbinina, E.A., Gavrilov, Y.O. (2015) Evidence for weathering and volcanism during the PETM from Arctic Ocean and Peri-Tethys osmium isotope records. *Palaeogeography, Palaeoclimatology, Palaeoecology* 438, 300–307, https://doi.org/10.1016/j.palaeo.2015.08.019

Dickson, A.J., Cohen, A.S., Davies, M. (2021) The osmium isotope signature of Phanerozoic Large Igneous Provinces. In: Ernst, R., Dickson, A.J., Bekker, A. (Eds) Large Igneous Provinces: a driver of global environmental and biotic changes. *AGU Geophysical Monograph Series* 255. https://doi.org/10.1002/9781119507444

Gleason, J.D., Thomas, D.J., Moore Jr, T.C., Blum, J.D., Owen, R.M., Haley, B.A. (2009) Early to middle Eocene history of the Arctic Ocean from Nd-Sr isotopes in fossil fish debris, Lomonosov Ridge. *Paleoceanography and Paleoclimatology* 24, PA2215, https://doi.org/10.1029/2008PA001685

Hutchinson, D.K., Coxall, H.K., O'Regan, M., Nilsson, J., Caballero, R., de Boer, A.M. (2019) Arctic closure as a trigger for Atlantic overturning at the Eocene–Oligocene transition. *Nature Communications* 10, 3797, https://doi.org/10.1038/s41467-019-11828-z

Jakobsson, M., Backman, J., Rudels, B., Nycander, J., Frank, M., Mayer, L., Jokat, W., Sangiorgi, F., O'Regan, M., Brinkhuis, H., King, J and Moran, K. (2007) The early Miocene onset of a ventilated regime in the Arctic Ocean. *Nature* 447, 986–990, https://doi.org/10.1038/nature05924

Levasseur, S., Birck, J-L., Allègre, C.J. (1998) Direct measurement of femtomoles of osmium and the $^{187}Os/^{186}Os$ ratio in seawater. *Science* 282, 272–274, https://doi.org/10.1126/science.282.5387.272

Levasseur, S., Birck, J-L., Allègre, C.J. (1999) The osmium riverine flux and the oceanic mass balance of osmium. *Earth and Planetary Science Letters* 174, 7–23, https://doi.org/10.1016/S0012-821X(99)00259-9

März, C., Schnetger, B., Brumsack, H-J. (2010) Paleoenvironmental implications of Cenozoic sediments from the central Arctic Ocean (IODP Expedition 302) using inorganic geochemistry. *Paleoceanography and Paleoclimatology* 25, https://doi.org/10.1029/2009PA001860

Moran, K., Backman, J., Brinkhuis, H., Clemens, S.C., Cronin, T., Dickens, G.R., Eynaud, F., Gattacceca, J., Jakobsson, M., Jordan, R.W., Kaminski, M., King, J., Koc, N., Krylov, A., Martinez, N., Matthiessen, J., McInroy, D., Moore, T.C., Onodera, J., O'Regan, M., Pälike, H., Rea, B., Rio, D., Sakamoto, T., Smith, D.C., Stein, R., St John, K., Suto, I., Suzuki, N., Takahashi, K., Watanabe, M., Yamamoto, M., Farrell, J., Frank, M., Kubik, P., Jokat, W., Kristoffersen, Y. (2006) The Cenozoic palaeoenvironment of the Arctic Ocean. *Nature* 441, 601–605, https://doi.org/10.1038/nature04800

O'Regan, M. (2008) Data report: high resolution bulk density, dry density, and porosity records from the Arctic Coring Expedition, IODP Expedition 302. In: Backman, J., Moran, K., McInroy, D.B., Mayer, L.A., Expedition 302 Scientists. *Proceedings of the IODP 302*. Integrated Ocean Drilling Program Management International, Inc., Edinburgh. https://doi.org/10.2204/iodp.proc.302.201.2008

Özsoy, E., Ünlüata, Ü (1997) Oceanography of the Black Sea: a review of some recent results. *Earth-Science Reviews* 42, 231–272, https://doi.org/10.1016/S0012-8252(97)81859-4

Pegram, W.J., Turekian, K.K. (1999) The osmium isotopic composition change of Cenozoic sea water as inferred from a deep-sea core corrected for meteoric contributions. *Geochimica et Cosmochimica Acta* 63, 4053–4058, https://doi.org/10.1016/S0016-7037(99)00308-7

Peucker-Ehrenbrink, B., Jahn, B. (2001) Rhenium-osmium isotope systematics and platinum group element concentrations: loess and the upper continental crust. *Geochemistry, Geophysics, Geosystems* 2, 2001GC000172, https://doi.org/10.1029/2001GC000172

Peucker-Ehrenbrink, B., Ravizza, G. (2000) The marine osmium isotope record. *Terra Nova* 12, 205–219. https://doi.org/10.1046/j.1365-3121.2000.00295.x

Peucker-Ehrenbrink, B., Ravizza, G., Hofmann, A.W. (1995) The marine $^{187}Os/^{188}Os$ record of the past 80 million years. *Earth and Planetary Science Letters* 130, 155–167. https://doi.org/10.1016/0012-821X(95)00003-U

Poirier, A., Hillaire-Marcel, C. (2009) Os-isotope insights in major environmental changes of the Arctic Ocean during the Cenozoic. *Geophysical Research Letters* 36, L11602, https://doi.org/10.1029/2009GL037422

Poirier, A., Hillaire-Marcel, C. (2011) Improved Os-isotope stratigraphy of the Arctic Ocean. *Geophysical Research Letters* 38, L14607, https://doi.org/10.1029/2011GL047953

Ravizza, G., Turekian, K.K., Hay, B.J. (1991) The geochemistry of rhenium and osmium in recent sediments from the Black Sea. *Geochimica et Cosmochimica Acta* 55, 3741–3752, https://doi.org/10.1016/0016-7037(91)90072-D

Roberts, C.D., LeGrande, A.N., Tripati, A.K. (2009) Climate sensitivity to Arctic seaway restriction during the early Paleogene. *Earth and Planetary Science Letters* 286, 576–585, https://doi.org/10.1016/j.epsl.2009.07.026

Stärz, M., Jokat, W., Knorr, G., Lohmann, G. (2017) Threshold in North Atlantic-Arctic Ocean circulation controlled by the subsidence of the Greenland-Scotland ridge. *Nature Communications* 8, 15681, https://doi.org/10.1038/ncomms15681

Stickley, C.E., St John, K., Koc, N., Jordan, R.W., Passchier, S., Pearce, R.B., Kearns, L.E. (2009) Evidence for middle Eocene Arctic sea ice from diatoms and ice-rafted debris. *Nature* 460, 376–379, https://doi.org/10.1038/nature08163

Sweere, T., van den Boorn, S., Dickson, A.J., Reichart, G-J. (2016) Definition of new trace-metal proxies for the controls on organic matter enrichment in marine sediments based on Mn, Co, Mo and Cd concentrations. *Chemical Geology* 441, 235–245, https://doi.org/10.1016/j.chemgeo.2016.08.028

Waddell, L.M., Moore, T.C. (2008) Salinity of the Eocene Arctic Ocean from oxygen isotope analysis of fish bone carbonate. *Paleoceanography and Paleoclimatology* 23, PA1S12, https://doi.org/10.1029/2007PA001451